

# Theory and Geometry of Constrained Cutting

S. I. Petrushin<sup>a</sup> and A. V. Proskokov<sup>b</sup>

<sup>a</sup>Tomsk Polytechnic University

<sup>b</sup>Yurginsk Technical Institute, a Branch of Tomsk Polytechnic University

**Abstract**—The geometric parameters of tools in constrained cutting are determined. A new dynamic coordinate system is proposed, and conversion formulas to other coordinate systems are presented. The cross section of the cut layer in constrained cutting is described.

**DOI:** 10.3103/S1068798X09110136

In modern manufacturing, the basic process is cutting, which is highly accurate and requires relatively little energy. At the same time, thanks to advances in the production process such that the size and shape of the blank are now close to those of the final part, cutting is now more of a finishing process. Cutting speeds have greatly increased, with considerable decrease in cross section of the cut layer. As a result, the working section of the cutting tool is the rounded tip of the blade. In other words, cutting is a more constrained process, on account of the greater curvature of the cutting edge.

In the present work, constrained cutting implies a process in which the deformation of the cut layer corresponds to a three-dimensional plastic-deformation source in the chip-forming zone. Most cutting methods are constrained. Their thorough investigation should permit the development of scientific machining principles. Attempts to create a theory of cutting extend throughout machining history and continue today [1]. Note that constrained oblique-angle cutting by a tool with a curvilinear cutting edge is the least developed process, although it is also the most common.

Before we consider the mechanics and physics of constrained cutting, we need to refine some key concepts regarding the region of direct tool–blank interaction. The working part of any metal-cutting tool is the blade (one or more), which removes the chip from the blank and directly experiences the cutting forces and thermal load. The blade surface in contact with the cut layer and chip is the front surface; the surface in contact with the surfaces of the blank is the rear surface. The line formed by the front and rear surfaces is the cutting edge. The point of the cutting edge that is introduced most deeply into the blank is the tip of the blade. For a curvilinear cutting edge, the division into primary and auxiliary sections is meaningless.

In investigating constrained cutting and determining the tool parameters, we use three rectangular coordinate systems [2]: the tool system, the static system, and the kinematic system. The tool coordinate system  $xyz$  (Fig. 1), with origin  $O$  at the tip of the blade, is oriented

with respect to the geometric elements of the cutting tool that form the basis. Since we will later assign a different meaning to the tool coordinate system, we refer here instead to the machine-tool coordinate system, which is oriented in the axial, radial, and tangential direction relative to the rotating blank or rotating tool. The origin of the static and kinematic coordinate systems is at point  $A$  of the cutting edge (which is curvilinear in the general case). The static system is oriented with respect to the direction of the primary cutting

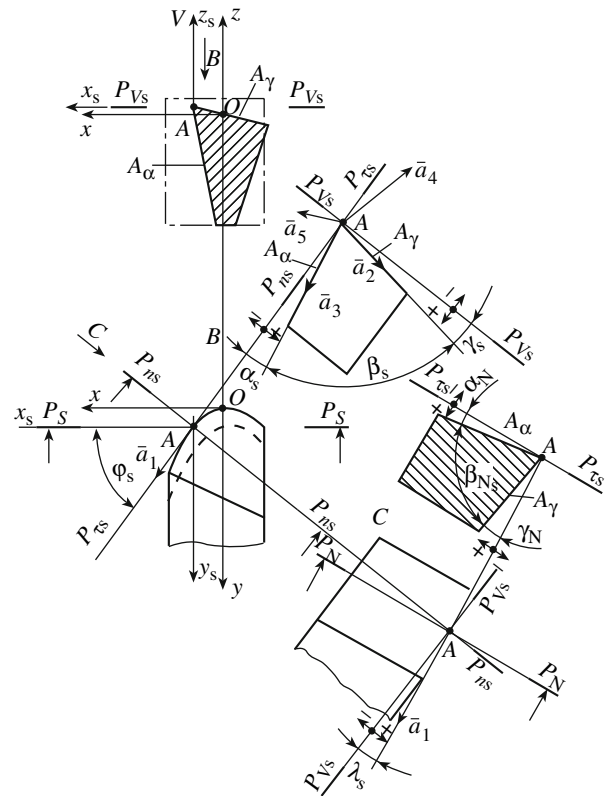


**Fig. 1.** Machine-tool and static coordinates for a curvilinear blade.

speed  $v$  (Fig. 1); the kinematic system is oriented with respect to the direction of the resultant cutting speed  $v_s$ .

To determine the blade geometry in the direction of chip departure, we introduce the dynamic coordinate system (Fig. 2): a rectangular coordinate system with its origin at a given point of the cutting edge, oriented with respect to the direction of initial chip departure in constrained cutting.

All the systems share the following (Figs. 1 and 2):

- the working plane  $P_S$ , in which the directions of the primary cutting speed and supply lie;
- the normal secant plane  $P_N$ , perpendicular to the cutting edge at the given point;
- the front blade surface  $A_\gamma$ , in contact with the cut layer and chip during cutting;
- the rear blade surface  $A_\alpha$ , in contact with the surfaces of the blank during cutting.

It follows from Fig. 1 that, for any tool, the machine tool  $(xyz)$  and static  $(x_s, y_s, z_s)$  coordinate systems have the same orientation; switching from one to the other involves parallel transfer of the  $xyz$  system from the blade tip  $O$  to point  $A$  of the curvilinear cutting edge, for which the geometric parameters are determined. To this end, three mutually perpendicular planes are constructed through point  $A$ :

- the primary static plane  $P_{vs}$ , perpendicular to the primary cutting speed  $v$ ;
- the static cutting plane  $P_{ts}$ , tangential to the cutting edge and perpendicular to the primary static plane  $P_{vs}$ ;
- the static primary secant plane  $P_{ns}$ , perpendicular to the line of intersection of the primary static plane  $P_{vs}$  and the static cutting plane  $P_{ts}$ .

In State Standard GOST 25762–83, incorrect assumptions were made in defining the cutting plane and the primary secant plane, in our view. Since the tangential plane is traditionally denoted by subscript 0 and the normal plane by subscript  $n$ , we will use this notation for the coordinate planes.

In view  $B$  (the top view of the blade), the static plane angle  $\varphi_s$  is defined as the angle in the primary static plane between the static cutting plane  $P_{ts}$  and the working plane  $P_S$ . If point  $A$  is to the right of point  $O$ , then  $\varphi_s$  is negative.

The primary static angles of the cutting wedge at point  $A$  are considered in the static primary secant plane  $P_{ns}$  and defined as follows:

- the static primary rear angle  $\alpha_s$  is the angle between the rear surface  $A_\alpha$  of the blade and the static cutting plane  $P_{ts}$ ;
- the static primary front angle  $\gamma_s$  is the angle between the front surface  $A_\gamma$  of the blade and the primary static plane  $P_{vs}$ ;
- the static primary sharpening angle  $\beta_s$  is the angle between the front  $A_\gamma$  and rear  $A_\alpha$  surfaces of the blade.

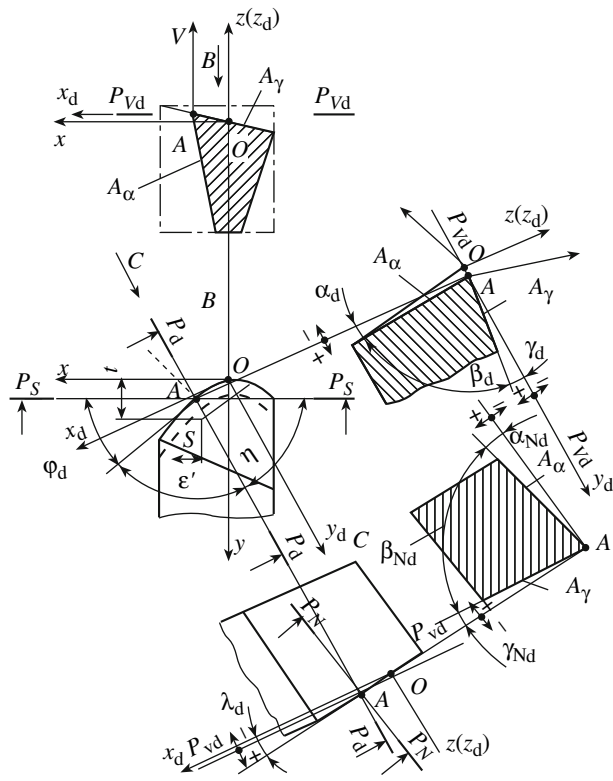


Fig. 2. Dynamic coordinate system.

By definition, the sum of  $\alpha_s$ ,  $\gamma_s$ , and  $\beta_s$  is  $\pi/2$ . The conventional signs of the angles  $\alpha_s$  and  $\gamma_s$  are shown in Fig. 1. If the front and rear surfaces of the blade are not plane, the angles between the tangents to the surfaces  $A_\alpha$  and  $A_\gamma$  at point  $A$  are considered.

View  $C$  permits definition of the natural static inclination  $\lambda_s$  of the edge as the angle in the static cutting plane  $P_{ts}$  between the cutting edge and the primary static plane  $P_{vs}$ . For a curvilinear cutting edge, the tangent in the plane of  $P_{ts}$  is constructed at point  $A$ . The signs for  $\lambda_s$  are shown in Fig. 1.

In the normal secant plane  $P_N$ , the static normal front angle  $\gamma_{Ns}$ , normal rear angle  $\alpha_{Ns}$ , and normal sharpening angle  $\beta_{Ns}$  (equal to  $\pi/2$ ) are defined.

The definitions for  $\varphi_s$ ,  $\alpha_s$ ,  $\gamma_s$ , and  $\lambda_s$  permit complete description of the blade geometry at any point of the cutting edge. The auxiliary angles  $\varphi_{1s}$ ,  $\alpha_{1s}$ ,  $\gamma_{1s}$ , and  $\lambda_{1s}$  are unnecessary. In the rectilinear sections of the cutting edge, they are the same for any point. The situation is more complex if complete description of the blade geometry is required in static coordinates—i.e., when both the cutting edge and the working surfaces are not plane. In that case, at least two different approaches are possible: (1) specification of the equations of the front  $A_\gamma$  and rear  $A_\alpha$  surfaces in the coordinates  $xyz$ , while the equation of the cutting edge corresponds to the line of intersection of these surfaces [3]; (2) numerical specification of the working-surface topography and computer description of the blade geometry [4]. Both

approaches permit description of blade geometry of any complexity. However, a deficiency of the first approach is the complexity of analytical description of the tool shape; a deficiency of the second is that approximate solutions are obtained. A third approach was proposed in [5, 6]. In that case, the mathematical apparatus of vector algebra is employed, as we will briefly outline.

Suppose that the equation of the cutting edge in the static coordinate system is specified in parametric form

$$\begin{cases} x = x(t); \\ y = y(t); \\ z = z(t). \end{cases} \quad (1)$$

At point  $A$ , we construct a tangent to the cutting edge. The unit directional vector  $\vec{a}_1$  of this tangent is specified by the expression

$$\vec{a}_1 = x'(t)\vec{i} + y'(t)\vec{j} + z'(t)\vec{k}, \quad (2)$$

where  $x'(t), y'(t), z'(t)$  are derivatives of Eq. (1).

On the other hand, by definition

$$\vec{a}_1 = \cos\lambda_s \cos\varphi_s \vec{i} + \cos\lambda_s \sin\varphi_s \vec{j} + \sin\lambda_s \vec{k}. \quad (3)$$

From Eqs. (2) and (3)

$$\begin{aligned} \varphi_s &= \arctan[y'(t)/x'(t)]; \\ \lambda_s &= \arcsin z'(t). \end{aligned}$$

The angles  $\gamma_s$  and  $\alpha_s$  specify the position of the front  $A_\gamma$  and rear  $A_\alpha$  surfaces in the static primary secant plane  $P_{ns}$  (Fig. 1). Then the corresponding unit directional vectors from point  $A$  are defined as follows:

for  $A_\gamma$

$$\vec{a}_2 = -\cos\gamma_s \sin\varphi_s \vec{i} + \cos\gamma_s \cos\varphi_s \vec{j} - \sin\gamma_s \vec{k};$$

for  $A_\alpha$

$$\vec{a}_3 = -\sin\alpha_s \sin\varphi_s \vec{i} + \sin\alpha_s \cos\varphi_s \vec{j} - \cos\alpha_s \vec{k}.$$

The position of the normal to the front surface at point  $A$  is defined by the vector

$$\begin{aligned} \vec{a}_4 &= \vec{a}_1 \times \vec{a}_2 \\ &= [(\cos\lambda_s \sin\gamma_s \sin\varphi_s + \sin\lambda_s \cos\gamma_s \cos\varphi_s)\vec{i} \\ &+ (\cos\lambda_s \sin\gamma_s \cos\varphi_s - \sin\lambda_s \cos\gamma_s \sin\varphi_s)\vec{j} \\ &+ \cos\lambda_s \cos\gamma_s \vec{k}] \times \sqrt{1 - \sin^2\lambda_s \sin^2\gamma_s}. \end{aligned}$$

while the normal to the rear surface is specified by the vector

$$\begin{aligned} \vec{a}_5 &= \vec{a}_4 \times \vec{a}_1 \\ &= [(\sin\alpha_s \sin\lambda_s \cos\varphi_s + \cos\alpha_s \cos\lambda_s \sin\varphi_s)\vec{i} \\ &+ (\sin\alpha_s \sin\lambda_s \sin\varphi_s - \cos\alpha_s \cos\lambda_s \cos\varphi_s)\vec{j} \\ &- \sin\alpha_s \cos\lambda_s \vec{k}] \times \sqrt{1 - \sin^2\lambda_s \sin^2\alpha_s}. \end{aligned}$$

The angles of the cutting wedge in the normal secant plane may be determined by means of formulas describing the geometry of a blade with a plane front surface at the given point of the cutting edge, in static coordinates [3]

$$\begin{aligned} \tan\alpha_N &= \tan\alpha_s / \cos\lambda_s; \\ \tan\gamma_N &= \tan\gamma_s \cos\lambda_s; \\ \beta_N &= \pi/2 - \alpha_N - \gamma_N. \end{aligned}$$

The dynamic coordinate system in Fig. 2 is used to solve the following problems:

- (a) transition from free cutting to constrained cutting;
- (b) determination of the front and rear angles and inclinations of the blade in the direction of chip departure from the front surface;
- (c) investigation of chip formation and twisting and also the stress and thermal stress at the blade in constrained cutting.

The initial parameter for the dynamic coordinate system is the angle of initial chip departure. The relevant GOST State Standard defines it as the angle (in the plane tangential to the front blade surface) between the direction of chip departure and the track of the primary secant plane. This definition cannot be regarded as adequate. For a curvilinear blade, there are different values of that angle at different points of the blade, whereas the chip has the same integral direction of departure. Therefore, another definition of the angle  $\eta$  of chip departure was proposed in [7]: the angle (in the basic dynamic plane  $P_{vd}$ ) between the secant plane  $P_s$  of chip departure and the working plane  $P_\eta$  (Fig. 2). The plane  $P_\eta$  passes through the direction of chip departure and the cutting speed.

Switching from the static system  $xyz$  to the dynamic coordinate system  $x_d y_d z_d$  entails counterclockwise rotation by  $\pi/2 - \eta$  around the axis  $Oz_d$  (Fig. 2). The new coordinates take the form

$$\left. \begin{aligned} x_d &= \sin\eta x + \cos\eta y; \\ y_d &= -\cos\eta x + \sin\eta y; \\ z_d &= z. \end{aligned} \right\} \quad (4)$$

Taking account of Eq. (4), we may express the directional vectors of the normals to the front ( $\vec{a}_4$ ) and rear ( $\vec{a}_5$ ) blade surfaces in the form

$$\begin{aligned} a_4 &= [\cos \lambda_s \sin \gamma_s \cos(\varphi_s + \eta) \\ &- \sin \lambda_s \cos \gamma_s \sin(\varphi_s + \eta)] \vec{i}_d + [\cos \lambda_s \sin \gamma_s \cos(\varphi_s + \eta) \\ &\times \vec{i}_d + [\cos \lambda_s \sin \gamma_s \cos(\varphi_s + \eta) \\ &+ \sin \lambda_s \cos \gamma_s \cos(\varphi_s + \eta)] \vec{j}_d + \cos \lambda_s \cos \gamma_s \vec{k}_d \cos \mu; \\ a_5 &= [\sin \alpha_s \sin \lambda_s \sin(\varphi_s + \eta) - \cos \alpha_s \cos \lambda_s \cos(\varphi_s + \eta)] \\ &\times \vec{i}_d - [\sin \alpha_s \sin \lambda_s \cos(\varphi_s + \eta) \\ &+ \cos \alpha_s \cos \lambda_s \sin(\varphi_s + \eta)] \vec{j}_d - \sin \alpha_s \cos \lambda_s \vec{k}_d \cos \mu, \end{aligned}$$

where  $\vec{i}_d, \vec{j}_d, \vec{k}_d$  are unit vectors of the dynamic coordinate system.

Note that, with the introduction of the dynamic coordinate system, the dynamic rear angle  $\alpha_d$  is no longer the primary characteristic of the contact conditions between the rear surface and the cutting surface at the blank, since the secant plane  $P_s$  of chip departure is perpendicular to the projection of the cutting edge onto the primary plane  $P_d$ , in the general case. To permit simultaneous consideration of processes at the front and rear surfaces in constrained cutting by a curvilinear blade, we must construct a discontinuous cross section through edge A: along the front surface to the edge parallel to plane  $P_s$  and then along the normal to the cutting edge (Fig. 2, dashed curve). For this reason, we speak of the cutting blade, rather than the cutting wedge, although that the term is often used elsewhere.

In constrained oblique-angle cutting by tools with a curvilinear cutting edge, the standard system of geometric parameters ( $\gamma, \lambda, \varphi, \varphi_1, \alpha, \alpha_1$ ) cannot retain their initial significance, since each point of the cutting edge corresponds to a set of angles, which are no longer constant for the whole blade. To obtain the minimum quantity of initial data for description of the geometry of a curvilinear blade, it is expedient to resort to the orientation of the tool's plane front surface proposed by Taylor [8]: the front surface is inclined at angle  $\gamma_x$  in the coordinate plane  $zOx$  and angle  $\gamma_y$  in the coordinate plane  $zOy$ . The orientation of the blade's front surface with positive values of these angles is illustrated in Fig. 3. Analogously to the terms adopted in the sketch,  $\gamma_x$  will be called the frontal angle, while  $\gamma_y$  is the profile angle. (According to Taylor, these would be the lateral inclination and the rear inclination [8].) For a nonplane front surface of complex configuration, these angles specify the orientation of the cutting plate in the housing (composite tools with interchangeable polymer inserts [6]).

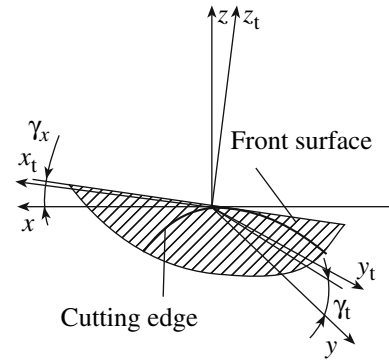


Fig. 3. Orientational angles of the blade's front surface.

As a result of double rotation, the initial (machine-tool) coordinate system  $xyz$  takes the position of the tool coordinate system  $x_t y_t z_t$  (Fig. 3), i.e., a rectangular coordinate system whose  $x_t O y_t$  plane is always in the plane of the blade's front (or supporting) surface. Conversion from one coordinate system to another is based on the formulas [5]

$$\left. \begin{aligned} x_t &= x \cos \gamma_x - y \sin \gamma_x \sin \gamma_y + z \sin \gamma_x \cos \gamma_y; \\ y_t &= y \cos \gamma_y + z \sin \gamma_y; \\ z_t &= -x \sin \gamma_x - y \cos \gamma_x \sin \gamma_y + z \cos \gamma_x \cos \gamma_y. \end{aligned} \right\} (5)$$

The following formulas permit conversion from the  $x_t y_t z_t$  system back to the  $xyz$  system

$$\left. \begin{aligned} x &= x_t \cos \gamma_x - z_t \sin \gamma_x; \\ y &= -x_t \sin \gamma_x \sin \gamma_y + y_t \cos \gamma_y - z_t \cos \gamma_x \sin \gamma_y; \\ z &= x_t \sin \gamma_x \cos \gamma_y + y_t \sin \gamma_y + z_t \cos \gamma_x \cos \gamma_y. \end{aligned} \right\} (6)$$

On the basis of Eqs. (5) and (6), we may switch from the proposed system of geometric parameters of the blade to the standard system. We find  $\lambda$  and  $\gamma$  from the formulas

$$\sin \lambda = \cos \varphi \sin \gamma_x + \sin \varphi \cos \gamma_x \sin \gamma_y; \quad (7)$$

$$\sin \gamma = \sin \varphi \sin \gamma_x - \cos \varphi \cos \gamma_x \sin \gamma_y. \quad (8)$$

Hence, for any point of the curvilinear cutting edge, we may find the inclination  $\lambda$  of the cutting edge and the primary front angle  $\gamma$  on the basis of the known plane angle  $\varphi$ , frontal angle  $\gamma_x$ , and profile angle  $\gamma_y$ .

According to Eqs. (7) and (8),  $\lambda$  and  $\gamma$  are specified by the same initial data. Therefore

$$\sin \gamma = \sin \lambda \tan \varphi - \cos \gamma_x \sin \gamma_y \sqrt{1 + \tan^2 \varphi}.$$

In Fig. 4, we plot the front angle and the inclination of the cutting edge as a function of the plane angle, in the radial part of the blade. Thus when the position of the front surface is specified by the frontal and profile angles, the geometry of the curvilinear blade at each

point is variable. Here  $\varphi$  is determined by the corresponding shape of the cutting edge, and  $\lambda$  and  $\gamma$  are not specified values but rather parameters to be calculated.

Using the proposed system, we may also perform appropriate transformation of the rear angles for a curvilinear blade in constrained oblique-angle cutting [6].

Thus, if we specify the equation of the cutting edge in the machine-tool or tool coordinate systems, constrained cutting by a curvilinear blade may be analyzed using the frontal angle  $\gamma_x$  and profile angle  $\gamma_y$ .

The switch from the tool system to the dynamic coordinate system is based on the formulas [4]

$$\left. \begin{aligned} x_d &= x_t(\cos\gamma_x \sin\eta - \sin\gamma_x \sin\gamma_y \cos\eta) + y_t \cos\gamma_y \cos\eta - z_t(\sin\gamma_x(\sin\eta + \cos\gamma_x \sin\gamma_y \cos\eta)); \\ y_d &= -x_t(\cos\gamma_x \cos\eta + \sin\gamma_x \sin\gamma_y \sin\eta) + y_t \cos\gamma_y \sin\eta + z_t(\sin\gamma_x \cos\eta - \cos\gamma_x \sin\gamma_y \sin\eta); \\ z_d &= x_t \cos\gamma_x \sin\gamma_y + y_t \sin\gamma_y + z_t \cos\gamma_x \sin\gamma_y \cos\gamma_y. \end{aligned} \right\} \quad (7)$$

The following formulas permit transition from the dynamic system back to the tool system

$$\left. \begin{aligned} x_t &= x_d(\cos\gamma_x \sin\eta - \sin\gamma_x \sin\gamma_y \cos\eta) - y_d(\cos\gamma_x \cos\eta + \sin\gamma_x \sin\gamma_y \sin\eta) + z_d \sin\gamma_x \cos\gamma_y; \\ y_t &= x_d \cos\gamma_y \cos\eta + y_d \cos\gamma_y \sin\eta + z_d \sin\gamma_y; \\ z_t &= -x_d(\sin\gamma_x \sin\eta + \cos\gamma_x \sin\gamma_y \cos\eta) + y_d(\sin\gamma_y \cos\eta - \cos\gamma_x \sin\gamma_y \sin\eta) + z_d \cos\gamma_x \cos\gamma_y. \end{aligned} \right\} \quad (8)$$

From Eq. (7), we may determine the dynamic front angle  $\gamma_d$  (Fig. 2) as the angle (in the secant plane  $P_s$  of

chip departure) between the axis  $y_d$  of the dynamic coordinate system and the front surface  $A_\gamma$

$$\cos\gamma_d = \pm\sqrt{\cos^2\gamma_y \sin^2\eta + (\cos\gamma_x \cos\eta + \sin\gamma_x \sin\gamma_y \sin\eta)^2}. \quad (9)$$

The dynamic inclination  $\lambda_d$  of the front surface is defined as the angle between axis  $x_d$  of the dynamic sys-

tem and the front surface  $A_\gamma$

$$\cos\lambda_d = \pm\sqrt{\cos^2\gamma_y \cos^2\eta + (\cos\gamma_x \sin\eta - \sin\gamma_x \sin\gamma_y \cos\eta)^2}. \quad (10)$$

According to Fig. 3, we take the minus sign ahead of the square root in Eq. (9) for  $\cos\gamma_d$ , and the plus sign in Eq. (10) for  $\cos\lambda_d$ .

Analysis of Eqs. (9) and (10) shows that  $\gamma_d$  and  $\lambda_d$  do not depend on the shape of the cutting edge. This is a

significant benefit of the proposed description of blade geometry in terms of the frontal and profile angles.

Constrained cutting may involve a single curvilinear blade, several linear blades, or a combination of linear and curvilinear cutting edges. The cross section of the cut layer depends on the plane geometry of the blade, the cutting kinematics, the cutting depth, and the supply.

A sharpened blade for external longitudinal turning with  $\gamma_x = \gamma_y = 0$  is shown in Fig. 5. Since  $\lambda = 0$ , this corresponds to constrained orthogonal cutting. The equations of the cutting edges in the machine-tool coordinate system take the form

$$\begin{cases} y = \tan\varphi x & \text{when } x \geq 0; \\ y = -\tan\varphi_1 x & \text{when } x < 0. \end{cases} \quad (11)$$

Here  $\varphi_1$  is the auxiliary plane angle.

The equations of the preceding position of the cutting edges are as follows

$$\begin{cases} y = \tan\varphi(x + S) & \text{when } x \geq -S; \\ y = -\tan\varphi_1(x + S) & \text{when } x < -S. \end{cases} \quad (12)$$

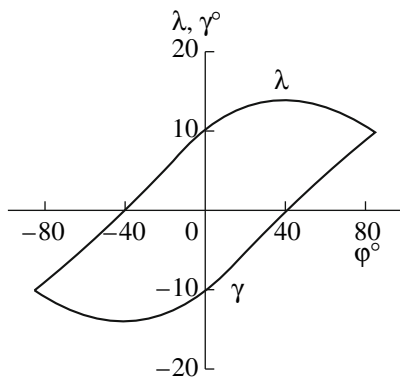


Fig. 4. Influence of the angle  $\varphi$  in the radial part of the blade on the angles  $\gamma$  and  $\lambda$ :  $\gamma_x = \gamma_y = 10^\circ$ .

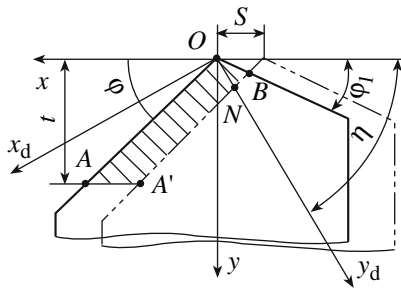


Fig. 5. Cross section of the cut layer for constrained orthogonal cutting by a sharpened blade.

The key points of the cut-layer cross section correspond to the coordinates

$$A\{t \cot \varphi; t\}; \quad A'\{t \cot \varphi - S; t\};$$

$$B\left\{-\frac{S \tan \varphi}{\tan \varphi + \tan \varphi_1}; \frac{S \tan \varphi \tan \varphi_1}{\tan \varphi + \tan \varphi_1}\right\}.$$

It follows from Fig. 5 that, with a long primary cutting edge, the thickness of the cut layer is constant, by definition

$$a = S \sin \varphi. \quad (13)$$

The width of the cut layer for the section of the cutting surface adjacent to the primary cutting edge is

$$b = t / \sin \varphi.$$

The area of the cut layer is determined by the area  $AOBA'$

$$f = tS - \frac{S^2 \tan \varphi \tan \varphi_1}{2(\tan \varphi + \tan \varphi_1)}.$$

In constrained cutting, we often consider the cross section of the cut layer in the direction of chip departure. Switching to the dynamic coordinate system on the basis of Eq. (7), we obtain the following key coordinates of the cut layer

$$\left. \begin{aligned} &A\{t(\sin \eta \cot \varphi + \cos \eta); t(\sin \eta - \cos \eta \cot \varphi)\}; \\ &B\left\{\frac{S \tan \varphi (\cos \eta \tan \varphi_1 - \sin \eta)}{\tan \varphi + \tan \varphi_1}; \right. \\ &\left. \frac{S \tan \varphi (\cos \eta + \tan \varphi_1 \sin \eta)}{\tan \varphi + \tan \varphi_1}\right\}; \\ &A'\{t(\cot \varphi \sin \eta + \cos \eta) - S \sin \eta; \\ &t(\sin \eta - \cot \varphi \cos \eta) + S \cos \eta\}. \end{aligned} \right\} (14)$$

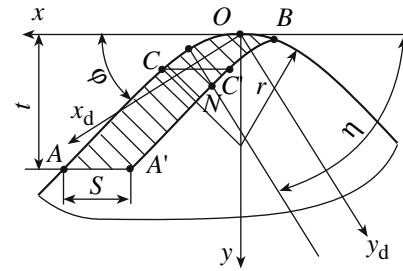


Fig. 6. Cut-layer cross section for a rounded blade.

The cut-layer thickness in the direction of chip departure varies as follows (Fig. 5): from point A to point A', it increases linearly from zero to the value

$$a = S \sin \varphi / \sin(\varphi + \eta). \quad (15)$$

Then the cut-layer thickness remains constant to point O, beyond which it declines linearly to zero at point B.

The total width of the cut layer from A to B is

$$b' = t(\sin \eta \cot \varphi + \cos \eta) - \frac{S \tan \varphi (\cos \eta \tan \varphi - \sin \eta)}{\tan \varphi + \tan \varphi_1}.$$

In the general case (Fig. 6), linear sections of the primary and secondary cutting blades are involved in cutting, as well as the rounded tip (radius  $r$ ).

The equations of the cutting edges in the  $xOy$  system take the form

$$y(x) = \begin{cases} \tan \varphi x + r(1 - \cos \varphi - t g \varphi \sin \varphi) & \text{when } x > r \sin \varphi; \\ r - \sqrt{r^2 - x^2} & \text{when } r \sin \varphi > x \geq -r \sin \varphi_1; \\ -\tan \varphi_1 x + r(1 - \cos \varphi_1 - \tan \varphi_1 \sin \varphi_1) & \text{when } x < -r \sin \varphi_1. \end{cases} (16)$$

The equations of the preceding position of the cutting edges take the form

$$\left. \begin{aligned} &y(x) \\ &= \begin{cases} \tan \varphi(x + S) + r(1 - \cos \varphi - \tan \varphi \sin \varphi) & \text{when } x > r \sin \varphi - S; \\ r - \sqrt{r^2 - (x + S)^2} & \text{when } r \sin \varphi > x > -r \sin \varphi_1 - S; \\ -\tan \varphi_1(x + S) + r(1 - \cos \varphi_1 - \tan \varphi_1 \sin \varphi_1) & \text{when } x < -r \sin \varphi_1 - S. \end{cases} \end{aligned} \right\} (17)$$



The coordinates of the key points (Fig. 6) are

$$A \left\{ \frac{(t-r)\cos\varphi+r}{\sin\varphi}; t \right\} \text{ when } t > r\cos\varphi;$$

$$A \{ \sqrt{2rt-t^2}; t \} \text{ when } t < r\cos\varphi;$$

$$A' \left\{ \frac{(t-r)\cos\varphi+r}{\sin\varphi} - S; t \right\} \text{ when } t > r\cos\varphi;$$

$$A' \{ \sqrt{2rt-t^2} - S; t \} \text{ when } t < r\cos\varphi;$$

$$C \{ r\sin\varphi; r(1-\cos\varphi) \};$$

$$C' \{ r\sin\varphi - S; r(1-\cos\varphi) \};$$

$$B \left\{ -\frac{S}{2}; r - \sqrt{r^2 - \frac{S^2}{4}} \right\}.$$

The area of the layer removed by the rounded tip is

$$f = S \left[ t - \frac{1}{3} \left( r - \sqrt{r^2 - \frac{S^2}{4}} \right) \right].$$

In the dynamic coordinate system, the coordinates of the key points take the form

$$x_{2A} = \begin{cases} \frac{(t-r)\cos\varphi+r}{\sin\varphi} \sin\eta + t\cos\eta \\ \text{when } t > r\cos\varphi; \\ \sqrt{2rt-t^2} \sin\eta + t\cos\eta \text{ when } t < r\cos\varphi; \end{cases}$$

$$y_{2A} = \begin{cases} \frac{(t-r)\cos\varphi+r}{\sin\varphi} \cos\eta + t\sin\eta \\ \text{when } t > r\cos\varphi; \\ -\sqrt{2rt-t^2} \cos\eta + t\sin\eta \text{ when } t < r\cos\varphi; \end{cases}$$

$$x_{2A'} = \begin{cases} \left[ \frac{(t-r)\cos\varphi+r}{\sin\varphi} - S \right] \sin\eta + t\cos\eta \\ \text{when } t > r\cos\varphi; \\ (\sqrt{2rt-t^2} - S) \sin\eta + t\cos\eta \\ \text{when } t < r\cos\varphi; \end{cases}$$

$$y_{2A'} = \begin{cases} \left[ S - \frac{(t-r)\cos\varphi+r}{\sin\varphi} \right] \cos\eta + t\sin\eta \\ \text{when } t > r\cos\varphi; \\ (S - \sqrt{2rt-t^2}) \cos\eta + t\sin\eta \\ \text{when } t < r\cos\varphi; \end{cases}$$

$$x_{2C} = r\sin\varphi\sin\eta + r(1-\cos\varphi)\cos\eta;$$

$$y_{2C} = -r\sin\varphi\cos\eta + r(1-\cos\varphi)\sin\eta;$$

$$x_{2C'} = (r\sin\varphi - S)\sin\eta + r(1-\cos\varphi)\cos\eta;$$

$$y_{2C'} = (S - r\sin\varphi)\cos\eta + r(1-\cos\varphi)\sin\eta;$$

$$x_{2B} = -\frac{S}{2}\sin\eta + \left( r - \sqrt{\frac{S^2}{4}} \right) \cos\eta;$$

$$y_{2B} = \frac{S}{2}\cos\eta + \left( r^2 - \sqrt{\frac{S^2}{4}} \right) \sin\eta.$$

As for a sharpened tip, the thickness  $a'$  of the cut layer is a variable; when  $t > r\cos\varphi$ , it is calculated from Eq. (15).

In considering chip formation, we cannot calculate cutting force, the cutting temperature, and the wear of the blade in constrained cutting unless we know the cut-layer cross section in the  $xOy$  plane and its projection onto the front surface of the tool. If we use Eq. (5) for a sharpened tip, the first relations in Eqs. (11) and (12) with  $z_t = 0$  will be

$$y_t = x_t \frac{\sin\gamma_x \sin\gamma_y + \tan\varphi \cos\gamma_x}{\cos\gamma_y}; \quad (18)$$

$$y_t = x_t \frac{\sin\gamma_x \sin\gamma_y + \tan\varphi \cos\gamma_x}{\cos\gamma_y} + \frac{S \tan\varphi}{\cos\gamma_y}. \quad (19)$$

Equations (18) and (19) describe the projections of the current and previous positions of the primary cutting edge on the plane front surface, whose position is specified by the frontal angle  $\gamma_x$  and profile angle  $\gamma_y$ . The distance between these positions along the normal determines the projection of the chip thickness  $a'$  onto the front surface

$$a' = \frac{S \tan\varphi_s}{\cos\gamma_y} \cos\varphi', \quad (20)$$

where

$$\varphi' = \arctan \frac{\sin\gamma_x \sin\gamma_y + \tan\varphi \cos\gamma_x}{\cos\gamma_y}.$$

When  $\gamma_x = \gamma_y = 0$ , Eq. (20) reduces to Eq. (13).

The direction of chip departure specified in the machine-tool coordinates  $xyz$  by the equation  $y = -x \tan\eta$  (Fig. 5) corresponds to a straight line in the plane of the front surface

$$y_3 = x_3 \frac{\sin\gamma_x \sin\gamma_y - \tan\eta \cos\gamma_x}{\cos\gamma_y}. \quad (21)$$

Solving Eqs. (21) and (18), we obtain the coordinates of point  $N$  (Fig. 6). Then the cut-layer thickness

$a'_1$  at the front surface in the direction of chip departure is determined by the length of segment  $MN$

$$a'_1 = \frac{S \tan \phi \sqrt{\cos^2 \gamma_y + (\cos \gamma_x \tan \eta - \sin \gamma_x \sin \gamma_y)^2}}{\cos \gamma_x \cos \gamma_y (\tan \phi + \tan \eta)}. \quad (22)$$

When  $\gamma_x = \gamma_y = 0$ , Eq. (22) reduces to Eq. (15).

For a curvilinear blade, the analytical formulas for the thickness of the cut layer in the direction of chip departure are complex. Therefore, it is expedient to use numerical methods, by specifying the position of point  $M$  of the blade (Fig. 6), through which we construct the line of chip departure, defined as

$$y - y_M = -\tan \eta (x - x_M). \quad (23)$$

Solving Eqs. (23) and (17), we obtain the coordinates of point  $N$  for the previous blade position. Then the thickness of the cut layer at point  $M$  is determined as the distance between these points

$$a' = \sqrt{(x_M - x_N)^2 + (y_N - y_M)^2}. \quad (24)$$

In Fig. 7, we present the results given by Eq. (24) for the thickness of the cut layer in the curvilinear section of the blade, at three values of the chip departure angle  $\eta$ . Obviously, with change in the direction of chip departure, not only the absolute thickness of the cut layer changes but also its variation along the blade; this does not entail any changes in the distribution of contact loads and thermal loads.

The projection of the cut-layer thickness  $a'_1$  onto the plane rear surface, which specifies the length of chip contact, is determined from Eq. (5), by switching to the coordinates of points  $M$  and  $N$ . Calculations show that the increase in  $a'_1$  relative to  $a'$  for the angles  $\gamma$  and  $\lambda$  is of no significance. Thus, with  $\pm 20^\circ$  variation in  $\gamma_x$ , the increase in  $a'_1$  is 3–4%. However, this difference must be taken into account when determining the contact length of the chip with the front surface and also for tools with large  $\lambda$  and  $\gamma$ .

The width of the cut layer, which specifies the chip width in constrained cutting by a rounded blade, is

$$b' = \begin{cases} \left[ \frac{(t-r)\cos\phi + r}{\sin\phi} + \frac{S}{2} \right] \sin\eta \\ + \left( t - r + \sqrt{r^2 - \frac{S^2}{4}} \right) \cos\eta \text{ when } t > r \cos\phi; \\ \left( \sqrt{2rt - t^2} + \frac{S}{2} \right) \sin\eta + \left( t - r + \sqrt{r^2 - \frac{S^2}{4}} \right) \cos\eta \\ \text{when } t < r \cos\phi. \end{cases}$$

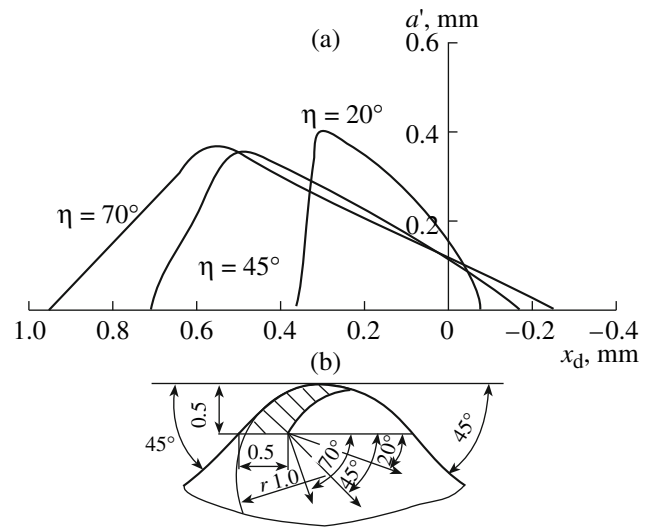


**Fig. 7.** Influence of the chip-departure angle  $\eta$  on the cut-layer thickness  $a'$  (a) and the process parameters (b):  $\phi = 45^\circ$ ;  $r = 1.0$  mm;  $S = 0.5$  mm/turn;  $t = 0.5$  mm.

Analogously, we may determine the parameters of the cut-layer cross section for cutting edges of any shape. In general, the coordinates of points of the edge may be specified.

REFERENCES

1. Vorontsov, A.L., Sultan-Zade, L.N., and Albagachiev, A.Yu., *New Theory of Cutting: Reference Materials and Applications*, *Inzh. Zh.*, 2007, no. 9, pp. 1–25.
2. *GOST (State Standard) 25762–83: Cutting: Terms, Definitions, and Notation for Common Concepts*, 1983.
3. Granovskii, G.I., *Kinematika rezaniya (Kinematics of Cutting)*, Moscow: Mashgiz, 1948.
4. Val'ter, A.V., *Software for Automated Analysis of Cutting Kinematics*, *Obrab. Met.*, 2008, no. 1, pp. 18, 19.
5. Petrushin, S.I., *Osnovy formoobrazovaniya rezaniem lezviinymi instrumentami (Principles of Shaping by Cutting Tools)*, Tomsk: Izd. TPU, 2003.
6. Petrushin, S.I., Bakanov, A.A., and Makhov, A.V., *Geometricheskii analiz konstruktii sbornikh rezhushchikh instrumentov so smennymi mnogrannymi plastinami (Geometric Analysis of the Design of Composite Cutting Tools with Interchangeable Polyhedral Plates)*, Tomsk: Izd. TPU, 2008.
7. Petrushin, S.I. and Proskokov, A.V., *Shape of the Curvilinear Tool Blade and Direction of Chip Departure in Oblique-Angle Cutting*, *Stanki Instrum.*, 2003, no. 12, pp. 26–29.
8. Taylor, F., *On the Art of Metal Cutting*, *ASME Trans.*, vol. 28, pp. 31–350, 1907.